

# Mechanical properties of suspended few layers graphene sheets

N. Sridi<sup>1</sup>, B. Lebental<sup>2,3</sup>, E. Merliot<sup>2</sup>, C. S. Cojocaru<sup>3</sup>, J. Azevedo<sup>4</sup>, J.J. Benattar<sup>4</sup>, A. Nowodzinski<sup>1</sup>, J.C.P. Gabriel<sup>1</sup> and A. Ghis<sup>1</sup>

<sup>1</sup>CEA-Grenoble, 17 rue des Martyrs, 38054 Grenoble Cedex 9, France, + 33 4 38 78 06 79

<sup>2</sup>Université Paris-Est, Ifsttar, 58 boulevard Lefebvre, 75732 Paris Cedex 15, France, +33 1 40 43 51 18

<sup>3</sup>LPICM Ecole Polytechnique, Route de Saclay, 91128 Palaiseau Cedex, France, +33 1 69 33 43 25

<sup>4</sup>Service de Physique de l'Etat Condensé, CEA-IRAMIS, 91191 Gif sur Yvette Cedex, France, +33 1 69 08 86 22

## ABSTRACT

In this paper, we present first a fabrication process of suspended graphene stripes. This process is done on a few layer graphene grown by CVD. In the second part, we introduce a new method to derive the value of the Young's modulus of ultrathin films using atomic force microscopy for experimental measurements and a continuum mechanics model for analytical fitting. Measurements are performed on few nanometers thick suspended graphene sheets grown by CVD.

**Keywords:** atomic force microscopy, mechanical properties, few layers graphene, graphene grown by CVD

## 1 INTRODUCTION

Graphene offers mechanical properties of potentially huge applicative interest, in particular for micro and nano electromechanical systems (MEMS and NEMS). The electromechanical behavior of a NEMS device (such as its resonance frequency) depends on the mechanical properties of the constituting materials [1]. We present here a method for the experimental determination of the mechanical properties of ultrathin films, whichever the material, and an application to a few layer graphene grown by CVD.

## 2 SAMPLE PREPARATION

### 2.1 Sample fabrication

#### a. Process outline

The test devices feature several pairs of parallel rectangular Cr/Au electrodes separated by 1.4 $\mu$ m. These electrodes are obtained by photo-lithography patterning and etching. They lie on a 200 nm thin SiO<sub>2</sub> layer deposited over a highly doped Si substrate. The films to be characterized are deposited onto the devices and then patterned into 20 $\mu$ m wide stripes. Finally, the underlying SiO<sub>2</sub> layer is chemically etched. As a result, the graphene sheets are suspended between pairs of metallic electrodes. A schematic of the fabrication process is shown in figure 1.

#### b. Graphene deposition

This process has been carried out on a single layer graphene grown by CVD and transferred onto the test device using a PMMA stamp [2]. After deposition, sheets appear corrugated.

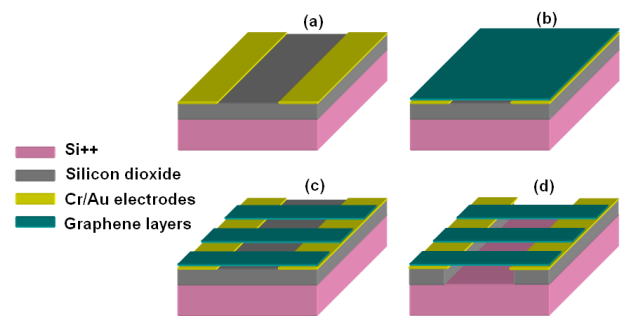


Figure 1: Fabrication steps. (a) 50nm thick Cr/Au electrodes separated by 1.4 $\mu$ m. (b) Graphene deposited over the test device. (c) Graphene stripes patterned and etched using oxygen plasma. (d) Suspended graphene stripes after chemical etching.

#### c. Graphene patterning

After graphene deposition, a positive photoresist is spread over the device by spin-coating. Photolithography is used to define 20  $\mu$ m wide resist stripes over graphene. Using oxygen plasma, graphene areas not covered by resist are etched away. Then the photo resist is removed by wet etching (AR 300-70 remover).

#### d. Graphene release by etching

To avoid surface tension effects likely to occur during wet HF etching, HF vapor is used to etch the silicon dioxide layer under the graphene sheets [3]. HF+H<sub>2</sub>O vapor is evaporated at room pressure and room temperature from a 49% HF/H<sub>2</sub>O solution.

SEM image of the suspended graphene structures is shown in figure 2. Graphene membrane appears partially suspended but not all along the 20 $\mu$ m of the stripe: it happens to be locally stuck at the bottom of the trench.

The typical suspended area is 1.4 $\mu$ m $\times$ 10 $\mu$ m. To our knowledge, this is the first time SiO<sub>2</sub> etch has been exploited to suspend graphene sheets over such dimensions. [5, 7, 10].

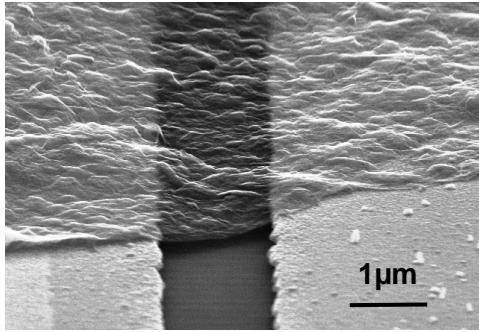


Figure 2: SEM image of a CVD few layers graphene sheet deposited using a PMMA stamp. Graphene sheet is suspended over a 200nm deep, 1.4 μm wide trench by SiO<sub>2</sub> etching.

## 2.2 Morphological characterization

Sheet roughness has been measured before SiO<sub>2</sub> etch using atomic force microscopy (AFM) in tapping mode. The thickness is only measured on the edges of the stripes because of the wrinkles. It ranges from 10nm to 14nm. We acquire height profiles perpendicularly to the axis of the trench using AFM in tapping mode; we can check that the SiO<sub>2</sub> layer is properly etched away where not covered by graphene. However, the actual removal of the oxide below the graphene sheet is not confirmed. We show later in this paper that AFM characterization in approach-withdrawal mode can confirm proper suspension.

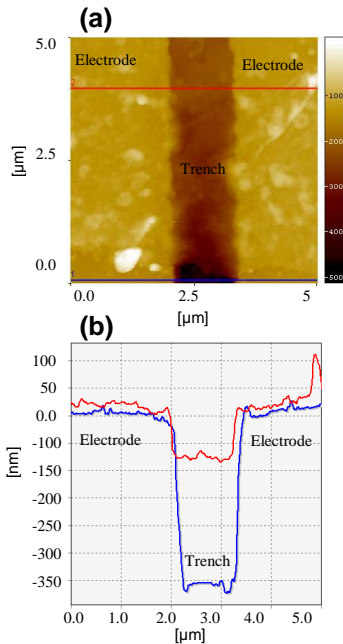


Figure 3: (a) AFM topography in tapping mode of a CVD graphene sheet. The trench is 300nm deep, 1.4 μm large. (b) Height profiles acquired along the blue (SiO<sub>2</sub>) and the red (graphene) lines of image (a).

## 3 AFM MEASUREMENTS OF ELASTIC PROPERTIES

### 3.1 Spring constant mapping

AFM is used in force-distance (approach-withdrawal) mode to estimate the elastic properties of the suspended membranes. The membrane is loaded by pushing the AFM cantilever down. Force-displacement curves (cantilever deflection versus vertical position) will be acquired and used to determine the membrane elastic properties.

#### a. Cantilever calibration

Sader's method is used to calculate the cantilever spring constant which depends on the cantilever size, first resonance frequency and quality factor according to the formula given in [4]. Its value is found to be  $k_c = 1.65$  N/m. The cantilever force sensitivity is obtained by acquiring force displacement curve away from the graphene sheet, on a hard bare surface (see figure 4). We assume the surface is not deformable, the indentation phenomena are neglected, and the slope of this curve yields the cantilever spring constant in V/nm. The averaged value over 320 measurements is  $S_c = 4 \times 10^6$  V/m.

From these two values, we deduce the cantilever force sensitivity is  $S_{f_c} = 2.42 \times 10^6$  V/N.

#### b. Effective spring constant mapping

We repeat the approach-withdrawal experiment on 32x32 points forming a grid over a 3μm x 3μm area of the test device. The scanned area contains a suspended CVD graphene sheet and part of the metallic electrodes on both sides of the suspended area. The corresponding values of the effective spring constant ( $k_{eff}$  in N/m) in each point are calculated using the previous force sensitivity of the cantilever  $S_{f_c}$ .

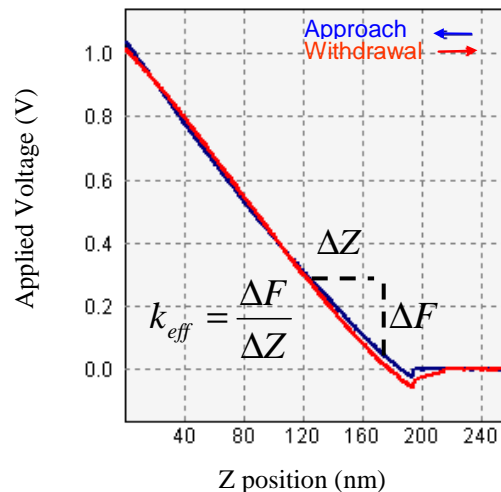


Figure 4: Force displacement curve (approach and withdrawal) obtained on a hard surface (i.e. an electrode). The effective spring constant of the whole cantilever-electrode system is calculated using the slope of the curve in the limit of small deflections.

### c. Membrane stiffness

For each point of the suspended area, the local equivalent spring constant ( $k_{eff}$ ) is a combination of both the cantilever and the membrane spring constants (eq. (1))

$$\frac{1}{k_{eff}} = \frac{1}{k_{gr}} + \frac{1}{k_c} \quad (1)$$

We can now calculate the local spring constant of the graphene sheet  $k_{gr}$ .

Figure 5 presents the equivalent spring constant values. This spring constant is significantly smaller where the graphene sheet is suspended than where it is stacked on the electrodes. Where the graphene lies stacked on the electrodes, the calculated spring constant corresponds to the combination of both the membrane and the hard surface electrode spring constants. This confirms that the membrane is well suspended over a  $1.4\mu\text{m}$  wide trench, in accordance with the SEM and AFM width measurements.

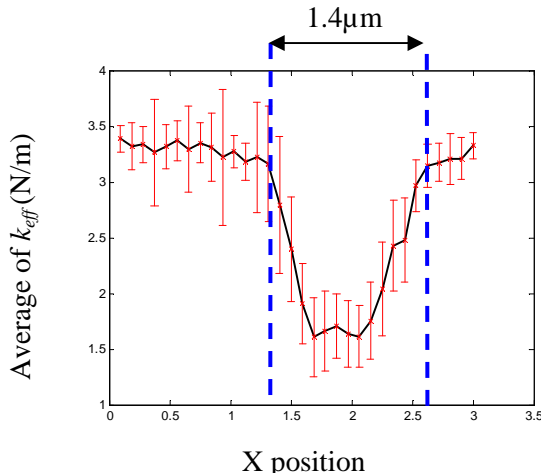


Figure 5: Profile of the average of the effective spring constant of a suspended CVD graphene sheet and electrodes across the trench.

## 3.2 Determination of Young's modulus

In the bibliography, the expression of the spring constant with respect to the mechanical coefficients is usually derived using continuum mechanics models. Calculations in references [5], [7] and [9] are for instance based on the model of a doubly clamped beam under a force applied at the center. It is however applicable only when the graphene stripes are very narrow ribbons (i.e. width much lower than suspended span).

In reference [6], the model of a circular plate with clamped edges derived in [11] is used; to our knowledge, neither the small nor the large deflection models of the rectangular plate with two opposite edges clamped and the two other edges free have ever been derived analytically. Hence, we have used finite element calculations to derive the

expression of the spring constant with respect to material parameters.

On the presented poster, we will present details of the calculation and discuss the resulting value of the Young modulus for the studied graphene membrane.

## 4 CONCLUSION

In this paper, a fabrication process to suspend graphene stripes has been described, and a method to estimate the Young's modulus has been presented. Measurements have been performed on few nanometers thick suspended graphene sheets grown by CVD.

The method to derive the value of the local Young's modulus is based on AFM experimental measurements and a continuum mechanics model for analytical fitting. We obtained a value of the Young's modulus  $E=0.12\pm 0.06$  TPa.

## REFERENCES

- [1] S.Timoshenko and J.N. Goodier. Theory of elasticity (1951). McGraw-Hill Book Company.
- [2] Baraton L., He Z. B. , Lee C. S., Cojocaru C. S., Chatelet M., Maurice J.-L., Lee Y. H. And Pribat D. "On the mechanisms of precipitation of graphene on nickel thin films" EPL-Europhys. Lett. 96 4 (2011).
- [3] Kirt R. Williams, Senior Member, IEEE, Kishan Gupta, Student Member, IEEE, and Matthew Wasilik, Journal of Microelectromechanical Systems, Vol.12, N° 6, December 2003.
- [4] J. E. Sader, J. W. M. Chon, P. Mulvaney, Rev. Sci. Instrum. 1999, 70, 3967.
- [5] Peng Li, Zheng You, Greg Haugstad, and Tianhong Cui, Appl. Phys. Lett. 98, 253105 (2011).
- [6] Castellanos-Gomez, A., Poot, M., Steele, G. A., van der Zant, H. S. J., Agraït, N. and Rubio-Bollinger, G. (2012). Adv. Mater., 24: 772–775.
- [7] Frank, I. W.; Tanenbaum, D. M.; van der Zande, A. M.; McEuen, P. L., Journal of Vacuum Science & Technology B: Microelectronics and Nanometer Structures (2007), vol. 25, issue 6, p. 2558
- [8] B.Kelly, Physics of Graphite (Applied Science, London; Englewood, NJ, 1981).
- [9] A. San Paulo, J. Bokor, R. T. Howe, R. He, P. Yang, D. Gao, C. Carraro, and R. Maboudian, Appl. Phys. Lett. 87, 053111 (2005)
- [10] Shriram Shivaraman, Robert A. Barton, Xun Yu, Jonathan Alden, Lihong Herman, MVS Chandrashekar, Jiwoong Park, Paul L. McEuen, Jeevak M. Parpia, Harold G. Craighead, and Michael G. Spencer, Nano Letters (2009), vol. 9, n° 9, p. 3100-3105.
- [11] Timoshenko, S.P. and S.Woinowsky-Krieger Theory of plates and shells, McGraw-Hill Book Company, Auckland, 1959.